Application of Two-Dimensional Conjugated Benzo[1,2-b:4,5-b']dithiophene in Quinoxaline-Based Photovoltaic Polymers

ARTICLE *in* MACROMOLECULES · APRIL 2012

Impact Factor: 5.8 · DOI: 10.1021/Ma300060z

Macromolecules

Article

pubs.acs.org/Macromolecules

Application of Two-Dimensional Conjugated Benzo[1,2-*b*:4,5-*b*′]dithiophene in Quinoxaline-Based Photovoltaic Polymers

Ruomeng Duan,[†,‡] Long Ye,[‡,§] Xia Guo,[‡,§] Ye Huang,[‡,§] Peng Wang,*[,†] Shaoqing Zhang,[‡] Jianping Zhang,[†] Lijun Huo,[‡] and Jianhui Hou*[,‡]

[†]Department of Chemistry, Renmin University of China, Beijing, 100872, China

[‡]State Key Laboratory of Polymer Physics and Chemistry, Institute of Chemistry, Chinese Academy of Sciences, Beijing 100190 China

[§]Graduate University of Chinese Academy of Sciences, Beijing 100049, China

Supporting Information

ABSTRACT: Two new donor−acceptor (D−A) alternative copolymers, PBDTDTQx-T and PBDTDTQx-O, were designed and synthesized to investigate the influence of two-dimensional conjugated structure on photovoltaic properties of conjugated polymers. In these two polymers, PBDTDTQx-O was used as control material, which is an alternative copolymer based on a quinoxaline derivative (DTQx) and alkoxy-substituted benzo[1,2-*b*:4,5-*b*′]dithiophene (BDT-O) unit; PBDTDTQx-T has an identical conjugated backbone as PBDTDTQx-O, but a simple two-dimensional conjugated BDT unit (BDT-T) was used to replace the alkoxy-BDT. The polymers were characterized by TGA, UV−vis absorption, electrochemical cyclic voltammetry, hole mobility of space-charge-limited current (SCLC) model, and photovoltaic measurements. It was found that PBDTDTQx-T exhibits similar molecular energy levels and higher hole mobility than PBDTDTQx-O. The power conversion efficiency (PCE) of the polymer solar cells (PSCs) based on PBDTDTQx-T: [6,6]-phenyl-C-71-butyric acid methyl ester ($PC_{71}BM$) = 1/2 (w/w) reached ∼5%, which is 60% higher than that of PBDTDTQx-O-based PSC. On the basis of these results, it can be concluded that the application of two-dimensional conjugated structure would be a feasible approach to improve photovoltaic properties of conjugated polymers.

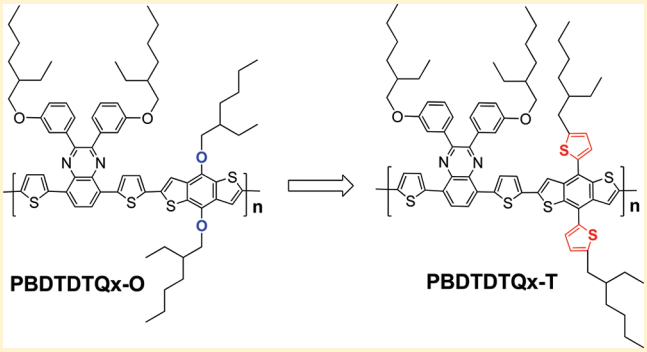

INTRODUCTION

Bulk-heterojunction (BHJ) polymer solar cells (PSCs) have attracted much attention due to its potential applications in making large area, flexible solar panels through roll-to-roll process.[1−6] In a PSC device with BHJ structure, the active layer is consisting of two kinds of key materials: a p-type conjugated polymer donor and a soluble fullerene derivative acceptor. In order to get efficient PSC devices, active layer materials with ideal properties are requisite, and therefore, tremendous efforts have been devoted to tuning the properties of active layer materials through molecular structure design.[7−11]

As electron donor materials in PSC devices, narrow band gap conjugated polymers are much helpful to obtain good harvest of the sunlight, and different strategies of molecular design have been developed. Building a donor−acceptor (D−A) alternating structure has been proved to be an effective way to reduce band gap of conjugated polymer materials.[12−19] For example, PCPDTBT[20,21] and PSBTBT[22] are two representatives with D−A structure, and these two polymers exhibit narrow band gaps (E_g < 1.6 eV) and promising photovoltaic properties (power conversion efficiency, PCE > 5%). Another effective way to reduce band gap of conjugated polymer is to introduce conjugating components with strong quinoid property.[23] For instance, conjugated polymers based on thieno[3,4-*b*]pyrazine (TPZ)[24] and thieno[3,4-*b*]thiophene (TT)[25−27] were designed and these polymers exhibit narrow band gaps and promising photovoltaic properties. Besides band gap control, the modulation of molecular energy levels (HOMO and LUMO) of conjugated polymers is also of great importance for photovoltaic material design. Electron donating or withdrawing functional groups have been used in molecular design for this purpose. For example, the alkoxy-substituted conjugated polymers show much higher HOMO levels than their analogues with alkyl-substituents due to the stronger electron donating ability of the alkoxy groups than the alkyls;[28] the carbonyl-substituted polymer exhibits lower LUMO level than the analogue with carboxylate group, because the carbonyl group has stronger electron withdrawing ability than the

Received: January 10, 2012
Revised: March 6, 2012
Published: March 20, 2012

Scheme 1. Molecular Structures of PBDTDTQx-O and PBDTDTQx-T

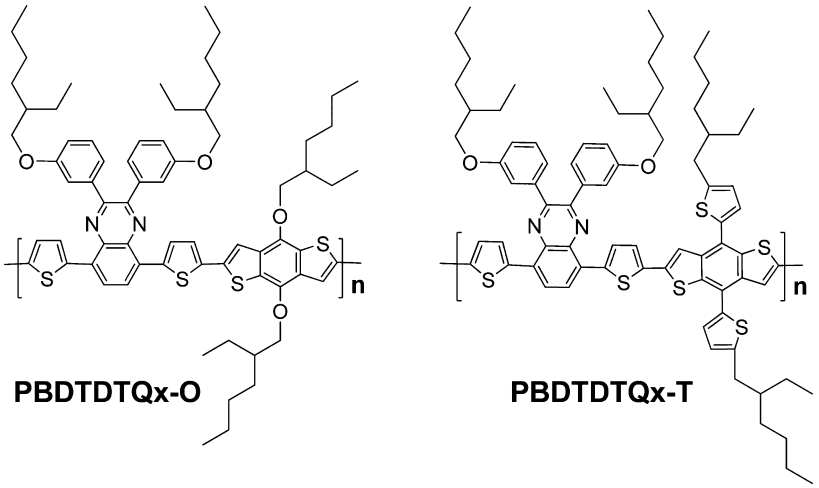

Scheme 2. Synthetic Route of PBDTDTQx-O and PBDTDTQx-T

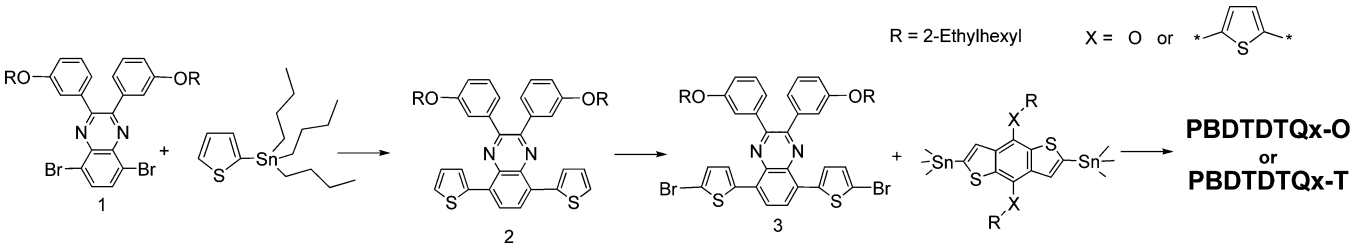

carboxylate;[25] the fluorine-substituted polymers also give excellent examples upon this strategy.[27,29]

Two-dimensional (2-D) conjugated polymers exhibit very interesting properties and promising photovoltaic performance. Representatively, intensive studies about 2-D-conjugated polythiophenes have been done.[30−33] 2-D-conjugated polythiophenes exhibit two main absorption peaks: one originates from the conjugated main chain, and the other is from the conjugated side chain. Consequently, broad and strong absorption band can be achieved in 2-D-conjugated polythiophenes.[30−32] On the other hand, since the 2-D-conjugated polythiophenes have bigger conjugated plane than their one-dimensional conjugated counterparts, better interchain $\pi-\pi$ overlapping can be formed and hence higher charge mobility can be achieved.[33] Recently, we designed and synthesized a new benzo[1,2-*b*:4,5-*b*′]dithiophene (BDT) derivative with 2-D-conjugated structure by introducing alkylthienyl groups to 4 and 8 positions of BDT unit. Initially, a polymer backbone (PBDTTT) was selected to investigate the photovoltaic properties of the 2-D-conjugated BDT-polymer. We found that after introducing 2-D-conjugated structure, broader absorption band, lower HOMO level and higher hole mobility can be achieved, and as a result, better photovoltaic results were recorded. For instance, PCE of the PSC devices based on the 2-D polymers, PBDTTT-E-T and PBDTTT-C-T, are 50% and 20% higher than their analogues with one-dimensional conjugated backbone, respectively.[34]

As known, the backbone of PBDTTT-based polymers has very strong quinoid property, so this kind of polymers exhibit much narrow band gaps.[34] Although it is quite clear that the 2-D-conjugated structure is very helpful to improving the photovoltaic properties of PBDTTT-based polymers, it is still unknown that how does the 2-D-conjugated structure influence photovoltaic properties of the D−A polymers without quinoid characteristic. Quinoxaline (Qx) is a typical electron-deficient conjugated unit due to the strong electronegativity of the two nitrogen atoms. Many conjugated polymers with D−A backbone have been designed by using Qx or its derivatives as electron-withdrawing building blocks in their backbones. These Qx-based polymers generally exhibit interesting photovoltaic behaviors, and ∼6% PCE has been reported in the polymers based on thiophene and quinoxaline.[35−37] Furthermore, since Qx consists of two fused six-member ring, when it was copolymerized with other conjugated components, the target polymer should have much less quinoid property than PBDTTT-polymers. Considering the above reasons, in order to investigate the influence of 2-D-conjugated BDT on photovoltaic properties of D−A conjugated polymers without quinoid property, two polymers based on Qx were designed. In Scheme 1, molecular structures of two D−A polymers based on BDT and the derivative of Qx, PBDTDTQx-O and PBDTDTQx-T, are shown, and these two polymers have identical conjugated backbones (main chain) but different side groups: alkoxy groups and alkylthienyl groups are used on 4 and 8 positions of their BDT units, respectively. Since these two polymers have similar molecular structures, the comparison between them will provide useful information on the influence of 2-D-conjugated structure on photovoltaic properties of D−A polymers.

RESULTS AND DISCUSSION

Synthesis. The general synthetic method of these two polymers is shown in Scheme 2. (2,3-Bis(3-(2-ethylhexyloxy)-phenyl)-5,8-di(thiophen-2-yl)quinoxaline (compound **2**) was synthesized by Stille condensation reaction between 5,8-Dibromo-2,3-bis(3-(2-ethylhexyloxy)phenyl)-quinoxaline

dx.doi.org/10.1021/ma300060z | *Macromolecules* 2012, 45, 3032−3038

(compound **1**) and 2-(tributylstannyl)thiophene with a yield of 60%, and then it was bromided by N-bromosuccininide (NBS) to produce compound **3**. The two target polymers were prepared through Stille polycondensation reaction with a yield of 40−60%. These two polymers exhibit excellent solubility in commonly used solvents, including tetrahydrofuran, chloroform, chlorobenzene, toluene, etc. Molecular weight of the polymers and polydispersity (PDI) was estimated by gel permeation chromatography (GPC) method using monodispersed polystyrene as standard and chloroform as eluent (Table 1). The number-average molecular weight (M_n) of PBDTDTQx-O and PBDTDTQx-T are 84K and 49.5K, respectively.

Table 1. Molecular Weight and Thermal Stability Data of the Polymers

polymer	M_w[a]	M_n[a]	PDI[a]	T_d (°C)
PBDTDTQx-O	186K	84K	2.22	320
PBDTDTQx-T	80.5K	49.5K	1.63	430

[a] M_w, M_n, and PDI of the polymers were estimated by GPC using polystyrene as standards in chloroform.

Thermal Properties. Thermal stability of the two polymers was investigated by thermogravimetric analysis (TGA). As shown in Figure 1, under nitrogen atmosphere, PBDTDTQx-O

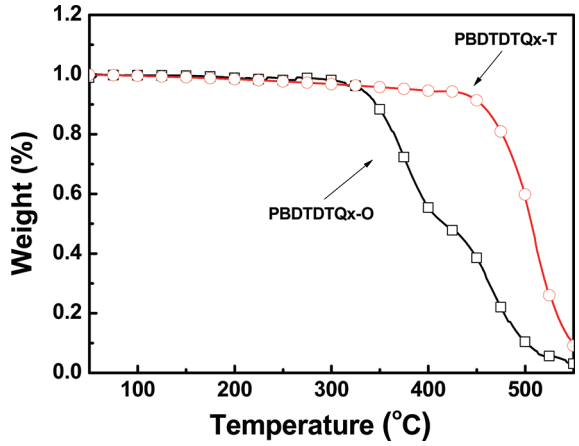

Figure 1. TGA plots of PBDTDTQx-T and PBDTDTQx-O with a heating rate of 10 °C/min under inert atmosphere.

shows an onset decomposition point at about 320 °C; however, PBDTDTQx-T shows an onset decomposition point at about 430 °C. The big difference of their decomposition temperature indicates that the 2-D-structure is much helpful to improving thermal stability of the BDT-based polymers. The difference scanning calorimetry (DSC) measurements for the two polymers have not shown any endothermic or exothermic phases in the temperature range of 25−300 °C. The DSC plots are shown in the Supporting Information (Figure S2).

Absorption Spectra. The absorption spectra of PBDTDTQx-O and PBDTDTQx-T in chloroform solution and of solid films are shown in Figure 2. As listed in Table 2, the absorption peaks of PBDTDTQx-O in solution and of solid film are at ~582 and ~602 nm, respectively; the absorption peaks of PBDTDTQx-T in solution and of solid film are both at ~605 nm. The absorption range of PBDTDTQx-T is red-shifted compared to PBDTDTQx-O. The absorption edges

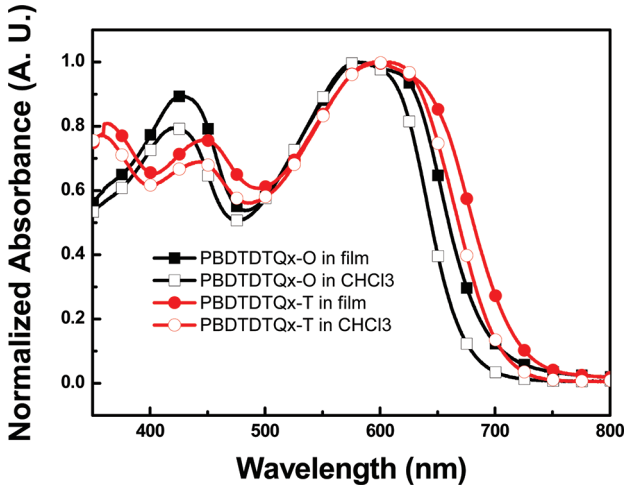

Figure 2. Absorption spectra of PBDTDTQx-T and PBDTDTQx-O in chloroform solution and of solid films.

(λ_{edge}) of PBDTDTQx-O and PBDTDTQx-T are located at 714 and 740 nm, corresponding to band gaps (E_g) of 1.74 and 1.67 eV, respectively; the half peak positions at long wavelength direction of PBDTDTQx-O and PBDTDTQx-T are 658 and 680 nm, respectively. PBDTDTQx-T exhibits a red-shifted absorption spectrum than PBDTDTQx-O indicating that the π-electrons of PBDTDTQx-T can be delocalized more effectively than that of PBDTDTQx-O, which is ascribed to the introduction of the 2-D conjugated structure. Besides of absorption range, absorption coefficient of solid film is also another important parameter to an active layer material in PSCs. As listed in Table 2, PBDTDTQx-O and PBDTDTQx-T exhibit much similar absorption coefficients as solid film, which are 0.60×10^{-2}/nm and 0.61×10^{-2}/nm, respectively. Since the 2-D conjugated polymer exhibits broader absorption band and similar absorption coefficient compared to the control polymer, when PBDTDTQx-T is used as active layer material in PSC, the device will harvest more photons than the PBDTDTQx-O-based device.

Electrochemical Properties. Electrochemical cyclic voltammetry (CV) is performed to evaluate molecular energy levels of conjugated polymers. Figure 3 shows the CV plots of PBDTDTQx-O and PBDTDTQx-T films on glassy carbon electrode. The onset points of *p*-doping process of PBDTDTQx-T and PBDTDTQx-O are both at 0.42 V, corresponding to a HOMO level of −5.12 eV. Since it is very hard to get a sharp n-doping signal for these two polymers, CV curves of p-doping process were only provided here, and the LUMO levels of the polymers were calculated by "LUMO = HOMO + E_g^{opt}". As known, V_{OC} of bulk heterojunction PSCs is directly proportional to the offset between HOMO level of the donor and LUMO level of the acceptor, and it can be concluded that the 2-D conjugated structure has no negative effect on V_{OC} of PSCs.

Photovoltaic Properties. The PSC devices with a structure of ITO/PEDOT−PSS (Clevios 4083)/polymer:$PC_{71}BM$/Ca/Al were fabricated to investigate the photovoltaic properties of these two polymers. *o*-Dichlorobenzene (*o*-DCB) was used to prepare the solution for spin-coating of active layer, and the concentration of the solution used in this work was 10 mg/mL (polymer/*o*-DCB). At first, different donor/acceptor (D/A) ratios, 1:1, 1:2, and 1:3, were scanned. We found that the optimal D/A ratio for both PBDTDTQx-O

dx.doi.org/10.1021/ma300060z | Macromolecules 2012, 45, 3032−3038

Table 2. Optical and Electrochemical Properties of PBDTDTQx-T and PBDTDTQx-O

	λ_{max} [nm]		λ_{edge} [nm]	absorption coefficient			
polymer	solution	film	film	film	E_g^{opt} [eV]	HOMO [eV]	LUMO [eV][a]
PBDTQx-T	443, 605	448, 605	740	0.61×10^{-2}/nm	1.67	−5.12	−3.45
PBDTQx-O	421, 582	428, 602	714	0.60×10^{-2}/nm	1.74	−5.12	−3.38

[a]LUMO = HOMO + E_g^{opt}.

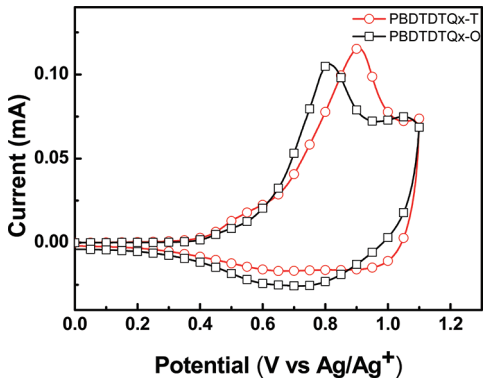

Figure 3. Cyclic voltammograms of PBDTDTQx-T and PBDTDTQx-O film on the glassy carbon electrode in 0.1 mol/L Bu_4NPF_6 in acetonitrile solution at a scan rate of 50 mV/s.

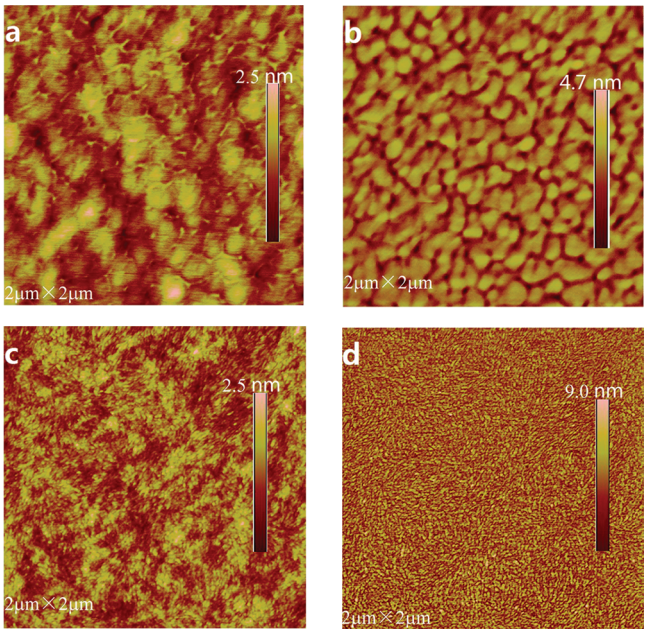

Figure 4. AFM images: (a, b) PBDTDTQX-O topography image and phase constrast image, respectively; (c, d) PBDTDTQX-T topography image and phase constrast image, respectively. All images are 2 μm × 2 μm.

and PBDTDTQx-T-based devices is 1/2, and Figure 5 shows the current−voltage curves (I−V curves) of the PSCs under illumination (AM1.5G 100 mW/cm^2). The detailed photovoltaic data of the optimization process of PBDTDTQx-T-based devices are listed in the Supporting Information as Table S1. It can be seen that the V_{OC} of PBDTDTQx-T-based devices dropped from 0.79 to 0.73 V with increasing $PC_{71}BM$ content in the blends, and the device with a D/A ratio of 1/2 showed the highest short circuit current density (J_{SC}) in these three conditions. As reported, device fabrication process of PSC can be further improved by thermal annealing[38,39] or by using 1,8-

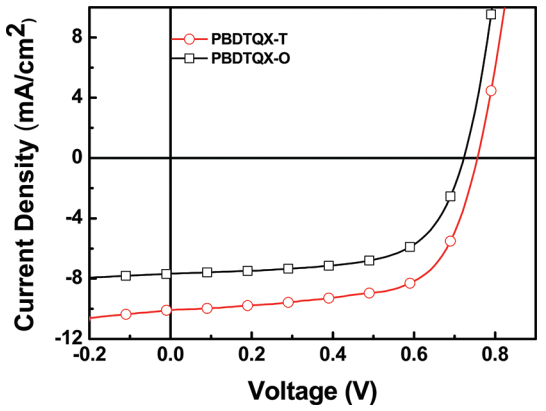

Figure 5. I−V curves of the PSCs based on PBDTDTQx-T and PBDTDTQx-O under the illumination of AM 1.5G, 100 mW/cm^2.

diiodooctane (DIO) as additive during the spin-coating process.[40] In this work, both of these two methods were employed to optimize the device performance. We found that no further improvement can be observed by using DIO as additive. However, after annealing at 120 °C, J_{SC} and fill factor (FF) of the devices can be improved simultaneously without affecting V_{OC}. In the optimized device, the thickness of the PEDOT−PSS layer is about 35 nm, the thicknesses of active layer are 80 and 126 nm for PBDTDTQX-T and PBDTDTQX-O-based devices, respectively. The thicknesses of Ca and Al layers are 20 and 80 nm, respectively. For PBDTDTQx-T-based device, a PCE of 4.95% was recorded with a V_{OC} of 0.76 V, a J_{SC} of 10.13 mA/cm^2 and a FF of 64.3%. Since PBDTDTQx-O has much similar structure as PBDTDTQx-T, the optimal device fabrication conditions of these two polymers are almost the same. However, both the V_{OC} and the J_{SC} of PBDTDTQx-O-based devices are lowered than PBDTDTQx-T-based devices, and therefore, the best PCE of the device of PBDTDTQx-O is only 3.06%. The nanoscale morphology of polymer/$PC_{71}BM$ film was tested by using atomic force microscopy (AFM). The phase graphs are shown in Figure 4. The surface roughness measured from the topograph image was 0.61 and 0.67 for PBDTDTQX-T and PBDTDTQX-O respectively. Although these two kinds of polymer:PCBM films show similar surface roughness, in comparison with the blend of PBDTDTQx-O and PCBM, the blend of PBDTDTQx-T exhibits much smaller domain size.

External Quantum Efficiency. As shown in Figure 6, the external quantum efficiency (EQE) curves of the devices indicate that the PSC devices have good response to the sunlight at the range from 350 to 700 nm, with a peak position at around 500 nm (Table 3). The EQE peak values of the PSC devices of PBDTDTQx-T and PBDTDTQx-O are 58% and 44%, respectively. PBDTDTQx-T-based device shows better EQE to the sunlight in the whole range compared to the PBDTDTQx-O-based device. This result indicates that the replacement of alkoxy group by alkylthienyl group is much

dx.doi.org/10.1021/ma300060z | Macromolecules 2012, 45, 3032−3038

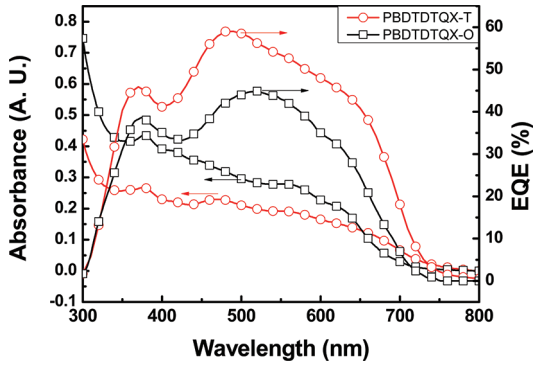

Figure 6. EQE curves of the PSCs based on PBDTDTQx-T or PBDTDTQx-O: $PC_{71}BM$ (1:2 w/w).

Table 3. Photovoltaic Properties of PSCs Based on PBDTDTQx-T and PBDTDTQx-O, under the Illumination of AM1.5G, 100 mW/cm^2

polymer	anneal (120 °C, 10 min)	D/A ratio	V_{OC} (V)	J_{SC} (mA/cm^2)	FF (%)	PCE (%)
PBDTDTQx-T	no	1:1	0.79	7.91	53.3	3.33
PBDTDTQx-T	no	1:2	0.76	8.97	50.5	3.44
PBDDTTQx-T	no	1:3	0.73	7.17	48.4	2.53
PBDTDTQx-T	yes	1:2	0.76	10.13	64.3	5.0
PBDTDTQx-O	yes	1:2	0.71	7.00	61.5	3.06

helpful to improve photovoltaic properties of the polymer. According to the EQE curves and the solar irradiation spectrum, the integral current density value of the PSC devices of PBDTDTQx-T and PBDTDTQx-O are calculated, which are 9.82 mA/cm^2 and 7.0 mA/cm^2, respectively. For both PBDTDTQx-T and PBDTDTQx-O-based devices, the difference between the measured J_{sc} and the integral current density values is within 4%, indicating the accuracy of our photovoltaic measurement is reliable.

Hole Mobility. Furthermore, hole mobilities of the D/A blend films based on these two polymers prepared by the optimal fabrication process were measured by fabricating hole-only device, the device structure as: ITO/PEDOT−PSS/polymer:$PC_{71}BM$/Au, and the results are shown in Figure 7. The hole mobilities of PBDTDTQx-T and PBDTDTQx-O are 1.04×10^{-4} cm^2 V^{-1} s^{-1} and 4×10^{-5} cm^2 V^{-1} s^{-1}, respectively. The higher hole mobility of PBDTDTQx-T than PBDTDTQx-O indicates that the replacement of alkoxy group by alkylthienyl group is an effective way to improve hole transport property of the active layer, and hence, better quantum efficiency can be obtained in the device based on the corresponding polymer with alkylthienyl side chain.

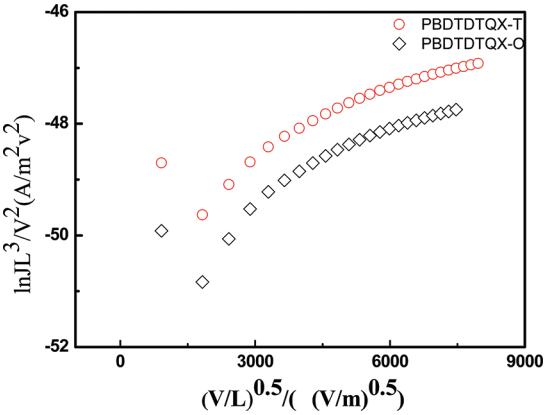

Figure 7. $\ln(JL^3/V^2)$ versus $(V/L)^{0.5}$ plots of the polymers for the measurement of hole mobility by the SCLC method.

CONCLUSION

Two new polymers based on Qx and BDT unit, PBDTDTQx-O and PBDTDTQx-T, were designed, synthesized and characterized. These two polymers exhibit broad absorption bands and appropriate molecular energy levels as electron donor materials in PSCs. Therefore, for the PSC device based on PBDTDTQx-T, a PCE of 5.0% were recorded. More important, two kinds of side groups, alkoxy group and alkylthienyl group, were used as substituents on the BDT units of these two polymers, and the comparison between them provides useful information for molecular design of photovoltaic polymers. The results in this work give solid evidence that the 2-D conjugated structure is beneficial to improve photovoltaic properties of the narrow band gap D/A-polymer system without quinoid properties. Specifically, after introducing the 2-D conjugated structure by replacing alkoxy groups with alkylthienyl groups, higher hole mobility and higher EQE of the PSC device was achieved, and therefore better J_{SC} can be realized; interestingly, although these two polymers exhibit similar HOMO levels, the PSC device based on 2-D conjugated polymer shows higher V_{OC} than the alkoxy-substituted control polymer. As a result, PCE of the device based on PBDTDTQx-T is ~60% higher than that of the device based on PBDTDTQx-O. Considering all the issues mentioned above, it can be concluded that the backbone of PBDTDTQx-T should be a promising molecular structure for photovoltaic polymer and the application of 2-D conjugated structure can be seen as a feasible method in molecular design of photovoltaic polymers.

EXPERIMENTAL SECTION

Materials. 2,6-Bis(trimethyltin)-4,8-bis(5-(2-ethylhexyl)thiophen-2-yl)benzo[1,2-*b*:4,5-*b*′]dithiophene (BDT-T), and 2,6-bis-(trimethyltin)-4,8-bis(2-ethylhexyloxy)benzo[1,2-*b*:4,5-*b*′]dithiophene (BDT-O); and the 5,8-dibromo-2,3-bis(3-(2-ethylhexyloxy)phenyl)-quinoxaline, were purchased from Solarmer Materials Inc. and used without any further purification. The $Pd(PPh_3)_4$ was purchased from Frontier Scientific Inc., and the ultra dry solvents used in device fabrication process are purchased from Aldrich. The other chemicals are commercial available products and used without any further purification.

Measurements. ^{1}H NMR spectra were measured on a Bruker arx-400 spectrometer. Absorption spectra were taken on a Hitachi U-3010 UV−vis spectrophotometer. The molecular weights of polymers were measured by the GPC method, and polystyrene was used as a standard by using chloroform as eluent. TGA measurements were performed on TA Instruments Inc. TGA-2050. Thermograms were obtained on mettle differential scanning calorimeter (DSC). The electrochemical cyclic voltammetry experiments were conducted on Zahner IM6e Eletrochemical workstation, with glassy carbon disk, Pt wire, and a Ag/Ag$^+$ electrode as the working electrode, counter electrode, and reference electrode, respectively, in a 0.1 mol/L tetrabutylammonium hexafluorophosphate (Bu_4NPF_6) in acetonitrile solution.

Synthesis. *2,3-Bis(3-(2-ethylhexyloxy)phenyl)-5,8-di(thiophen-2-yl)quinoxaline (**2**).* 2-(Tributylstannyl)thiophene(2.24 g, 6 mmol), compound **1** (1.40 g, 2 mmol), and 14 mL of toluene were put into a flask. The solution was purge with argon for 10 min, then 100 mg $Pd(PPh_3)_4$ was added. The solution was purge again by argon for 30 min the resulting mixture was

dx.doi.org/10.1021/ma300060z | *Macromolecules* 2012, 45, 3032−3038

heated with stirring at 110 °C for 12 h under argon atmosphere. Then the reactant was cooled to room temperature and then poured into water and extracted by diethyl ether for several times. After removal of the solvent, the crude product was purified by silica gel chromatography with hexane/dichloromethane (v/v, 5/1) mixture as eluent. The pure compound (2) was obtained as red solid (yield 60%). ^{1}H NMR (δ/ppm, $CDCl_3$, 400 MHz): 8.15 (s, 2H), 7.90 (d, 2H), 7.49 (d, 2H), 7.41 (s, 2H), 7.28 (t, 4H), 7.20 (t, 2H), 6.95 (d, 2H), 3.8 (d, 4H), 1.71 (m, 2H), 1.34 (m, 16H), 0.94 (t, 12H).

*2,3-Bis(3-(2-ethylhexyloxy)phenyl)-5,8-bis(5-bromothiophen-2-yl)quinoxaline (**3**).* To a solution of compound **2** (1.16 g, 1.65 mmol) in 10 mL *N*,*N*-dimethylformamide (DMF), a solution of *N*-bromosuccinimide (NBS) (0.60 g, 3.37 mmol) in 10 mL of DMF was added at 0 °C. The reactant was stirred for 30 min and then poured into water and extracted with diethyl ether (50 mL × 3). The organic phase was dried over anhydrous $MgSO_4$. After removal the solvent under reduced pressure, the residues were purified by silica gel column chromatography using hexanes as eluent. The pure product compound **3** was obtained as deep red solid in a yield of 94% (1.33 g). ^{1}H NMR (δ/ppm, $CDCl_3$, 400 MHz): 8.25 (s, 2H) 7.73 (d, 2H), 7.46 (s, 2H), 7.31 (t, 2H), 7.20 (t, 4H), 7.05 (d, 2H), 3.92 (d, 4H), 1.75 (m, 2H), 1.36 (m, 16H), 0.96 (t, 12H).

Synthesis of the Polymers Using Stille Coupling Reaction. Both PBDTDTQx-T and PBDTDTQx-O were prepared by coupling compound **3** with the corresponding bis(trimethylstannyl)-substituted BDT monomer by the same procedure. BDT-T (0.452 g, 0.5 mmol) or BDT-O (0.386 g, 0.5 mmol) and compound **3** (0.430 g, 0.5 mmol) were put into a 50 mL two-neck flask, and 10 mL of degassed toluene was added under the protection of argon. The solution was purge with argon for 10 min, and then 10 mg of $Pd(PPh_3)_4$ was added. After being purged with argon for 20 min, the reaction mixture was heated with stirring at 105 °C for 16 h. Then the reactant was cooled to room temperature, and the polymer was precipitated by adding methanol and then filtered through a Soxhlet thimble, which was then subjected to Soxhlet extraction with methanol, hexane, and chloroform successively. The polymer was recovered from the chloroform fraction by rotary evaporation as solid. The solid was dried under vacuum for 1 day. The yields of the two polymers were both about 40%.

Device Fabrication and Measurements. Polymer solar cell devices were fabricated under conditions as follows: After spin-coating a 35 nm layer of poly(3,4-ethylenedioxythiophene):poly(styrenesulfonate) (PEDOT:PSS) onto a precleaned indium−tin oxide (ITO) coated glass substrates, the polymer/$PC_{71}BM$ blend solution was spin-coated. The concentration of the polymer/$PC_{71}BM$ blend solution for spin-coating was 10 mg/mL (polymer/*o*-dichlorobenzene). The thickness of the active layer was controlled by changing the spin speed during the spin-coating process and measured on profilometer (Ambios Tech. XP-2). The devices were completed by evaporating Ca/Al metal electrodes with an area of 4 mm^2 as defined by masks. The *I*−*V* curves are measured under the illumination of 100 mW· cm^{-2} AM 1.5G using a XES-70S1 (SAN-EI Electric Co., Ltd.) solar simulator (AAA grade, 70 mm ×70 mm photobeam size). The 2 × 2 cm monocrystalline silicon reference cell (SRC-1000-TC-QZ) was purchased from VLSI Standards Inc.

■ ASSOCIATED CONTENT

Ⓢ Supporting Information

Optimizing of PBDTDTQx-base devices, differential scanning calorimetrythermograms, density functional theory calculations, and XRD patterns. This material is available free of charge via the Internet at http://pubs.acs.org.

■ AUTHOR INFORMATION

Corresponding Author

*E-mail: (J.H.) hjhzlz@iccas.ac.cn; (W.P.) wpeng@chem.ruc.edu.cn.

Notes

The authors declare no competing financial interest.

■ ACKNOWLEDGMENTS

The authors would like to acknowledge the financial support from National High Technology Research and Development Program 863, Chinese Academy of Sciences, NSFC (Nos. 2011AA050523, 20874106, 20821120293, 51173189, and 20933010).

■ REFERENCES

(1) Yu, G.; Gao, J.; Hummelen, J. C.; Wudl, F.; Heeger, A. J. *Science* **1995**, *270*, 1789−1791.
(2) Hoth, C. N.; Choulis, S. A.; Schilinsky, P.; Brabec, C. J. *Adv. Mater.* **2007**, *19*, 3973−3974.
(3) Aernouts, T.; Aleksandrov, T.; Girotto, C.; Genoe, J.; Poortmans, J. *Appl. Phys. Lett.* **2008**, *92* (3), 033306.
(4) Brabec, C. J.; Sariciftci, N. S.; Hummelen, J. C. *Adv. Funct. Mater.* **2001**, *11*, 15−26.
(5) Thompson, B. C.; Frechet, J. M. J. *Angew. Chem., Int. Ed.* **2008**, *47*, 58−77.
(6) Park, S. H.; Roy, A.; Beaupre, S.; Cho, S.; Coates, N.; Moon, J. S.; Moses, D.; Leclerc, M.; Lee, K.; Heeger, A. J. *Nat. Photo* **2009**, *3*, 297−U5.
(7) Cheng, Y. J.; Yang, S. H.; Hsu, C. S. *Chem. Rev.* **2009**, *109*, 5868−5923.
(8) Giacalone, F.; Martin, N. *Chem. Rev.* **2006**, *106*, 5136−5190.
(9) Roncali, J. *Chem. Rev.* **1992**, *92*, 711−738.
(10) Li, C.; Liu, M. Y.; Pschirer, N. G.; Baumgarten, M.; Mullen, K. *Chem. Rev.* **2010**, *110*, 6817−6855.
(11) He, Y. J.; Li, Y. F. *Phys. Chem. Chem. Phys.* **2011**, *13*, 1970−1983.
(12) Amb, C. M.; Chen, S.; Graham, K. R.; Subbiah, J.; Small, C. E.; So, F.; Reynolds, J. R. *J. Am. Chem. Soc.* **2011**, *133*, 10062−10065.
(13) Price, S. C.; Stuart, A. C.; Yang, L. Q.; Zhou, H. X.; You, W. *J. Am. Chem. Soc.* **2011**, *133*, 4625−4631.
(14) He, Z. C.; Zhong, C. M.; Huang, X.; Wong, W. Y.; Wu, H. B.; Chen, L. W.; Su, S. J.; Cao, Y. *Adv. Mater.* **2011**, *23*, 4636−4637.
(15) Liang, Y. Y.; Xu, Z.; Xia, J. B.; Tsai, S. T.; Wu, Y.; Li, G.; Ray, C.; Yu, L. P. *Adv. Mater.* **2010**, *22*, E135−136.
(16) Su, M. S.; Kuo, C. Y.; Yuan, M. C.; Jeng, U. S.; Su, C. J.; Wei, K. H. *Adv. Mater.* **2011**, *23*, 3315−3316.
(17) Blouin, N.; Michaud, A.; Gendron, D.; Wakim, S.; Blair, E.; Neagu-Plesu, R.; Belletete, M.; Durocher, G.; Tao, Y.; Leclerc, M. *J. Am. Chem. Soc.* **2008**, *130*, 732−742.
(18) Beaujuge, P. M.; Pisula, W.; Tsao, H. N.; Ellinger, S.; Mullen, K.; Reynolds, J. R. *J. Am. Chem. Soc.* **2009**, *131*, 7514−7515.
(19) Huang, F.; Chen, K. S.; Yip, H. L.; Hau, S. K.; Acton, O.; Zhang, Y.; Luo, J. D.; Jen, A. K. Y. *J. Am. Chem. Soc.* **2009**, *131*, 13886−13887.
(20) Peet, J.; Kim, J. Y.; Coates, N. E.; Ma, W. L.; Moses, D.; Heeger, A. J.; Bazan, G. C. *Nat. Mater.* **2007**, *6*, 497−500.
(21) Muhlbacher, D.; Scharber, M.; Morana, M.; Zhu, Z. G.; Waller, D.; Gaudiana, R.; Brabec, C. *Adv. Mater.* **2006**, *18*, 2884−2889.
(22) Yang, Y.; Hou, J. H.; Chen, H. Y.; Zhang, S. Q.; Li, G. *J. Am. Chem. Soc.* **2008**, *130*, 16144−16145.
(23) Huo, L. J.; Hou, J. H. *Polym. Chem.* **2011**, *2*, 2453−2461.
(24) Zhou, E. J.; Cong, J. Z.; Yamakawa, S.; Wei, Q. S.; Nakamura, M.; Tajima, K.; Yang, C. H.; Hashimoto, K. *Macromolecules* **2010**, *43*, 2873−2879.
(25) Hou, J. H.; Chen, H. Y.; Zhang, S. Q.; Chen, R. I.; Yang, Y.; Wu, Y.; Li, G. *J. Am. Chem. Soc.* **2009**, *131*, 15586−15587.
(26) Liang, Y. Y.; Wu, Y.; Feng, D. Q.; Tsai, S. T.; Son, H. J.; Li, G.; Yu, L. P. *J. Am. Chem. Soc.* **2009**, *131*, 56−57.
(27) Hou, J. H.; Chen, H. Y.; Zhang, S. Q.; Liang, Y. Y.; Yang, G. W.; Yang, Y.; Yu, L. P.; Wu, Y.; Li, G. *Nat. Photo* **2009**, *3*, 649−653.
(28) Shi, C. J.; Yao, Y.; Yang, Y.; Pei, Q. B. *J. Am. Chem. Soc.* **2006**, *128*, 8980−8986.

(29) Zhou, H. X.; Yang, L. Q.; Stuart, A. C.; Price, S. C.; Liu, S. B.; You, W. *Angew. Chem., Int. Ed.* **2011**, *50*, 2995−2998.
(30) Hou, J. H.; Tan, Z. A.; Yan, Y.; He, Y. J.; Yang, C. H.; Li, Y. F. *J. Am. Chem. Soc.* **2006**, *128*, 4911−4916.
(31) Hou, J. H.; Huo, L. J.; He, C.; Yang, C. H.; Li, Y. F. *Macromolecules* **2006**, *39*, 594−603.
(32) Hou, J. H.; Tan, Z.; He, Y. J.; Yang, C. H.; Li, Y. F. *Macromolecules* **2006**, *39*, 4657−4662.
(33) Li, Y. F.; Zou, Y. P. *Adv. Mater.* **2008**, *20*, 2952−2958.
(34) Huo, L. J.; Zhang, S. Q.; Guo, X.; Xu, F.; Li, Y. F.; Hou, J. H. *Angew. Chem., Int. Ed.* **2011**, *50*, 9697−9702.
(35) Wang, E. G.; Hou, L. T.; Wang, Z. Q.; Hellstrom, S.; Zhang, F. L.; Inganas, O.; Andersson, M. R. *Adv. Mater.* **2010**, *22*, 5240−5244.
(36) Gadisa, A.; Mammo, W.; Andersson, L. M.; Admassie, S.; Zhang, F.; Andersson, M. R.; Inganas, O. *Adv. Funct. Mater.* **2007**, *17*, 3836−3842.
(37) Zhou, E.; Cong, J. Z.; Tajima, K.; Hashimoto, K. *Chem. Mater.* **2010**, *22*, 4890−4895.
(38) Zhang, M. J.; Guo, X.; Li, Y. F. *Adv. Energy Mater.* **2011**, *1*, 557−560.
(39) Verploegen, E.; Mondal, R.; Bettinger, C. J.; Sok, S.; Toney, M. F.; Bao, Z. A. *Adv. Funct. Mater.* **2010**, *20*, 3519−3529.
(40) Lee, J. K.; Ma, W. L.; Brabec, C. J.; Yuen, J.; Moon, J. S.; Kim, J. Y.; Lee, K.; Bazan, G. C.; Heeger, A. J. *J. Am. Chem. Soc.* **2008**, *130*, 3619−3623.